PEROVMSKITE-OXIDES $Ba_xSr_{3-x}NbO_{5.5}$ (x = 0, 1 AND 2) COMPETENT FOR REMOVAL OF METHYL VIOLET FROM AQUEOUS SOLUTIONS

I. PARREY

Department of Chemistry, Periyar University Salem Tamil Nadu, India,
imtiyazchemistry@gmail.com, mobile phone: +91-9797855613

Abstract. Three members of the A-site doped Nb perovskites with general formula $Sr_3NbO_{5.5}$, $BaSr_2NbO_{5.5}$ and $Ba_2SrNbO_{5.5}$ were synthesized by solid-state methods and their removal efficiency of methyl violet from aqueous solutions was investigated. The X-ray diffraction measurements demonstrated that the three samples have a cubic faced perovskite-type structure in space group *Fmm.* The addition of Ba^{2+} into the A-site of $Sr_3NbO_{5.5}$ has influenced the cell volume, crystal size and density. Subsequently, the removal capacity was also impacted. The crystallite size of the oxides was determined to be less than 82 nm. The maximum removal capacities of methyl violet are found to be 46.5, 13.1 and 8.0 mg/g, using $Ba_2SrNbO_{5.5}$, $BaSr_2NbO_{5.5}$ and $Sr_3NbO_{5.5}$, respectively. The amounts of the dye adsorbed by the oxides have increased as the Ba^{2+} content increased. The removals of methyl violet have positive relationship with pH, temperature and the mass of the oxides.

Key words: Removal of methyl violet, A-site doping.

INTRODUCTION

The enormous increase in organic water pollution has generated a broad interest in developing new materials for environmental catalysis applications [16]. The family of perovskite-type oxides is one of promising materials for organic dye removal [14]. It is considered to be an adsorbent and catalytic for such process. Perovskite oxides with their flexible ABO_3 composition, where A is a rare earth metal with large ionic radius or alkali earth metals and B is a transition metal with a small ionic radius, offer immense possibilities in terms of adaptation to control their properties and functionalities [7]. Oxygen and cation non-stoichiometry can be tailored in a large number of perovskite compositions to achieve the desired catalytic activity, including multifunctional catalytic properties [13]. A key feature of perovskite-type catalysts is that a number of transition metals show excellent catalytic activity for a variety of reactions due to their electronic structure [15]. For

Received: July 2020;
In final form September 2020.

ROMANIAN J. BIOPHYS., Vol. 30, No. 4, P. 000–000, BUCHAREST, 2020

instance, O_2 adsorption on doped perovskites such as $La_{1-x}Sr_xCoO_3$ display two adsorption peaks (α and β). These peaks are attributed to adsorbed oxygen at low temperature and lattice oxygen at high temperature, respectively. The amount of O_2 adsorption and the intensity of α-type adsorption peak are related to non-stoichiometry and structural defect, where the decrease in α-type adsorption temperature is consistent with increasing in d electrons of the transition metals. The β type adsorption peaks is associated with B site cations [5].

This work studies the removal of methyl violet (MV) from aqueous solutions using $Ba_xSr_{3-x}NbO_{5.5}$ (x = 0, 1, 2). The $Sr_{3-x}Ba_xNbO_{5.5}$ oxides adopt a faced centered double cubic perovskite structure with space group *Fmm* and exhibit 1:1 cation ordering [2]. The high polarizing cations Sr^{2+} and Ba^{2+} fairly occupy the octahedral site obtaining a rocked salt ordering in the structure [10]. The ordered-cation distribution is attributed to the differences in both the ion size and the bonding character of the B-site cations. The title double perovskites display anomalous thermal expansion of the lattice parameters as a consequence of local clustering of the vacancies and/or the anions with absorbed water molecules [1]. The partial substitution of Sr^{+2} (12 coordinate ionic radius, 1.44 Å [12]) by Ba^{2+} (1.61 Å [12]) was expected to influence structural characteristics leading to changes in the adsorption properties. The physical properties of such oxides can be influenced by the differences in the effective charges, the ionic radii and the electron configurations of both the A and B-site cations.

Methyl violet 10B is known in medicine as gentian violet and is the active ingredient in a Gram stain, used to classify bacteria [18]. It is used as a pH indicator, with a range between 0 and 1.6. Compounds related to methyl violet are potential carcinogens. Methyl violet 10B inhibits the growth of many Gram-positive bacteria, except streptococci [4]. It is soluble in water, ethanol, diethylene glycol and dipropylene glycol. Methyl violet is a mutagen and mitotic poison, therefore concerns exist regarding the ecological impact of the release of methyl violet into the environment [18]. Methyl violet has been used in vast quantities for textile and paper dyeing, and 15 % of such dyes produced worldwide are released to environment in wastewater [3].

MATERIAL AND METHODS

EXPERIMENTAL

Sample preparation

The preparation of samples involved Nb_2O_5 (Merck, 99.99 %), $SrCO_3$ and/or $BaCO_3$ (BDH, 99.98–99.99 %). The appropriate stoichiometric amounts were mixed, using a mortar and pestle, and then heated in several steps with intermittent regrinding. Samples were initially heated at 850 °C for 12 h followed by reheating at 1100 °C for 48 h [6].

INSTRUMENTATIONS

The crystallography of the samples was examined by a PANalytical X'Pert X-ray powder diffraction using Cu Kα radiation (1.5400 Å) and a PIXcel solid-state detector. The operating voltage was 40 kV and the current was 30 mA. The samples were measured in lat plate mode at room temperature with a scan range of $10° < 2\theta < 80°$ and a scan length of 10 mins were used. The structures were refined using the program RIETICA [17].

The absorbance of solutions was determined using ultraviolet/visible spectrophotometer (UV/Vis, model Spect-21D) and (190-900 Perkin-Elmer) at maximum absorbance wavelength, 590 nm. The concentrations of solutions were estimated from the concentration dependence of fit. The pH measurements were carried out on a WTW720 pH meter model CT16 2AA (LTD Dover Kent, UK) and equipped with a combined glass electrode.

BATCH MODE

Batch mode removal studies were carried out by varying several parameters such as contact time, pH, temperature and mass of prepared oxide (adsorbent). Essentially, a 50 mL of dye solution with concentration of 10 ppm was taken in a 250 mL conical flask in which the initial pH was adjusted using HCl/NaOH. Optimized amount of adsorbent was added to the solution and stirred using magnetic stirrer for specific time. The oxide samples were separated from solutions using centrifuge 3500 CPM for 5 minutes.

RESULT AND DISCUSSIONS

CHARACTERIZATION OF OXIDES

Initially, our synthetic attempts focused on $Sr_{3-x}Ba_xNbO_{5.5}$ oxides where x = 0, 1, 2, and 3, however only for the three first compositions were single phase samples obtained. X-ray diffraction measurements (Fig. 1) demonstrated the three samples to be free of any obvious impurities and have a cubic faced structure with space group (*Fmm*). Doping with Ba^{2+} significantly increases both the cell volume and the density but decreases the crystallite size. The increase in cell volumes is likely driven by the large ionic size of the Ba^{2+} cation (12 coordinate ionic radius, 1.61 Å). The ionic size of the Sr^{2+} cation (12 coordinate ionic radius, 1.44 Å) is smaller than the Ba^{2+} cation. $BaSr_2NbO_{5.5}$ displayed the lowest crystallite size in the series, possibly as a consequence of cation order effects. The materials can be formulated as $(BaSr)SrNbO_{5.5}$ in order to emphasize the ordering at the B site between the Sr^{2+} and Nb^{5+} cations. In the double perovskite structure, it is anticipated that the two smallest cations will order in the octahedral sites, this ordering being a consequence of the differences in the size and/or charge between

the two cations. The largest cation will then occupy the 12-coordinate (cuboctahedral) site. The corresponding ionic radii of Ba^{2+} (12 coordinate ionic radius, 1.61 Å and 6 coordinate ionic radius. 1.35 Å [12]); Sr^{2+} (1.44 and 1.18 Å [12]) and Nb^{5+} (6 coordinate ionic radius. 0.64 Å [9]) cations suggest that the Nb^{5+} and one Sr^{2+} cation will occupy the 6-coordinate sites whereas a mixture of Sr^{2+} and Ba^{2+} will occupy the cuboctahedral sites [8].

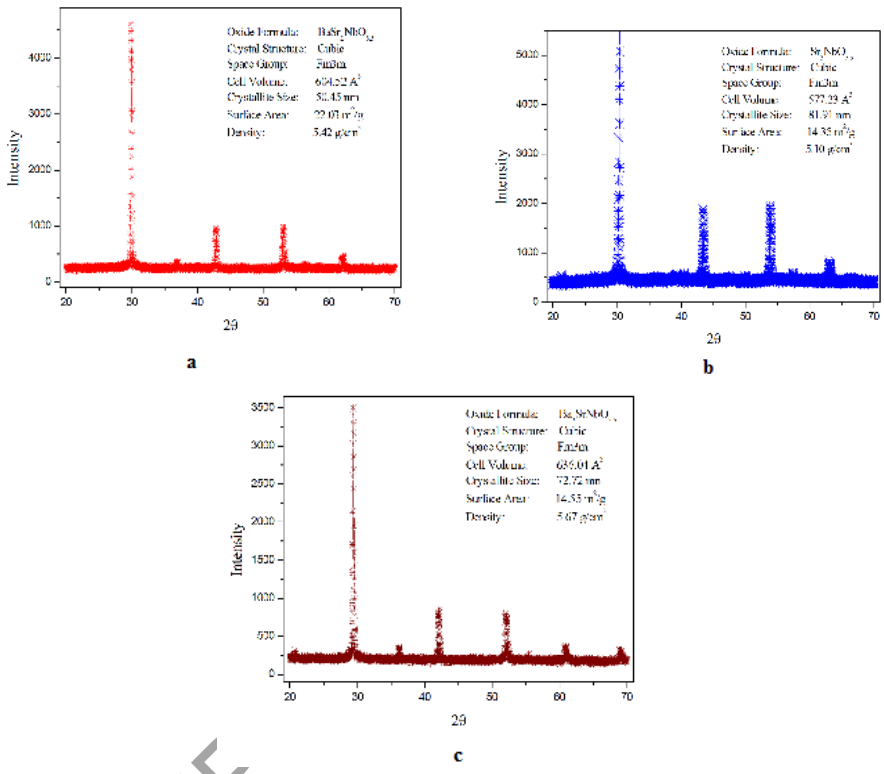

Fig. 1. The XRD patterns of: a. $Sr_3NbO_{5.5}$, b. $BaSr_2NbO_{5.5}$ and c. $Ba_2SrNbO_{5.5}$. θ is the angle between incident rays and reflected rays, in degrees. The intensity is in arbitrary units.

The average crystallite size D_p, the specific surface area S, the lattice strain φ, the lattice parameter a, the and cell volume V estimated from X-ray diffraction data are summarized in Table 1. The crystallite size can be calculated using Sheerer formula [9] (Eq. 1), where λ is the wavelength of rays, $\beta_{1/2}$ is the structural broadening between sample and standard, and θ is the angle between reflected rays and incident rays. The specific surface area can be calculated using Sauter formula [11] (Eq. 2), in which ρ is the density of the synthesized material.

$$D_p = 0.94\lambda/(\beta_{1/2} \times \cos\theta) \quad (1)$$

$$S = 6000/ (D_p \times \rho) \quad (2)$$

Table 1

Table indicates average crystallite size D_p, specific surface area S, lattice strain φ, lattice parameter a and cell volume V, estimated from X-ray diffraction data

Formula	D_p (nm)	ρ(g/cm3)	S (m2/g)	φ	a (Å)	V (Å3)
$Sr_3NbO_{5.5}$	81.91	5.104	14.35	0.0028	8.3263 (pH = 3)	577.230 (pH = 1)
$BaSr_2NbO_{5.5}$	50.45	5.419	22.03	0.0020	8.4554 (pH = 2)	604.520 (pH = 1)
$Ba_2SrNbO_{5.5}$	72.72	5.669	14.55	0.0020	8.5999 (pH = 3)	636.040 (pH = 2)

BATCH MODE

Effect of time

The removal percentage of dyes over the adsorbents can be calculated as:

$$R\% = [(C_i - C_t)/C_i] \times 100 \quad (3)$$

where R% is the removal percentage, C_i = 10 ppm is the initial concentration of dye solution, C_t is the concentration of dye at contact time, estimated from the concentration dependence of absorbance fit.

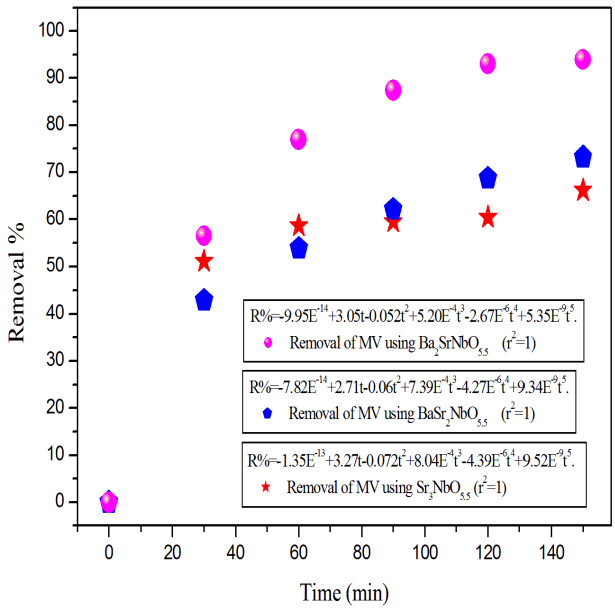

Fig. 2. The time dependence of MV removal at room temperature. The volume, concentration, and pH of the dye solution are 50 mL, 10 ppm and 5.1, respectively. E is the Langmuir constant and r_2 is the correlation coefficient.

Figure 2 shows the time dependence of MV removal at room temperature. There no finite time was observed for the dye removal up to 150 min. The removals of the dye increase as the contact time increases. The removal of MV on the surface of $Sr_3NbO_{5.5}$, $BaSr_2NbO_{5.5}$ and $Ba_2SrNbO_{5.5}$ were found to be 66.15, 73.24 and 93.94 %, respectively. The removal of MV using $Ba_2SrNbO_{5.5}$ was larger than those using $BaSr_2NbO_{5.5}$ and $Sr_3NbO_{5.5}$. This is due to the effect of oxide composition. The increase in the organic dye removal is consistent with the increase in the Ba^{2+} ion content. The inserted equations in Figure 2 describe the removal percentage (R%) as function of time (t) for each oxide. The initial removal rate (dR/dt) could be derived from the equations at t = 0. The initial removal rates for MV dye were found to be 3.25, 2.71, and 3.04 using $Sr_3NbO_{5.5}$, $BaSr_2NbO_{5.5}$ and $Ba_2SrNbO_{5.5}$, respectively. The wavelength dependence of absorbance for MV solution (Fig. 3) illustrates the absorbance of MV solutions decreased as result of using $Ba_xSr_{3-x}NbO_{5.5}$ oxides as adsorbents. In addition, the absorbance decreases as the value of x in the formula increased.

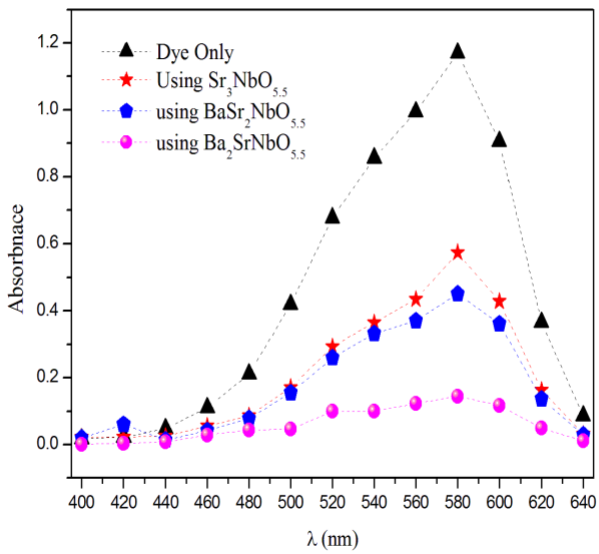

Fig. 3. The wavelength dependence of absorbance for MV solution. The time, volume, concentration, adsorbent mass and pH of MV solution are 150 min, 50 mL, 10 ppm, 0.1 g and 5.1, respectively.

Effect of adsorbent mass

The amount of the dye adsorbed by one gram of the oxides (Q) was calculated as following:

$$Q\ (\text{mg/g}) = [(C_i - C_t)\times V]/W \qquad (4)$$

where t = 150 min is the contact time, V = 50 mL is the volume of MV solution, and W is the mass of oxides.

As shown in Figure 4, Q decreases as the mass of adsorbents increased. The maximum capacity of adsorbent Q_{max} can be estimated from the intercept of the liner fit of $1/Q_t$ at y axis. $Ba_2SrNbO_{5.5}$ (72.72 nm, 14.55 m_2/g) displayed the highest value of $Q_{max,}$ 46.47 mg/g (pH = 2), whereas $Sr_3NbO_{5.5}$ (81.91 nm, 14.35 m_2/g) exhibited the lowest value of $Q_{max,}$ 8.03 mg/g (pH = 5). Q_{max} for $BaSr_2NbO_{5.5}$ (50.45 nm, 22.03 m_2/g) is 13.09 mg/g (pH = 2). This result suggested that an enhancement in the adsorption properties occurs as result of the substitution of Ba^{2+} into the oxide plus the decrease in crystallite size. The decrease in crystallite size leads to an increase in the surface area of particles.

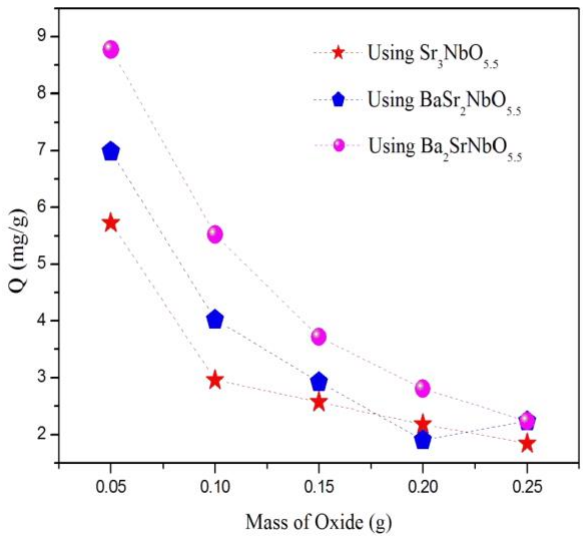

Fig. 4. The effect of adsorbent mass on the removal. The time, volume, concentration and pH of dye solutions are 150 min, 50 mL, 10 ppm and 5.1, respectively.

Effect of temperature

Temperature has an important impact on the adsorption process. An increase in temperature helps the reaction to compete more efficiently with e_-/H_+ recombination. The removal of two dyes was investigated at 25, 40, 60 and 100 ^oC. The obtained results are illustrated below in Figure 5. The removal of MV dye increased as temperature increased. For instance, the removal of MV increased from ~64.9 % at 25 ^oC to ~99 % at 100 ^oC when $BaSr_2NbO_{5.5}$ was used. This result is in agreement with normal expectations and is a consequence of the increase of adsorption strength and the concentration of active intermediates with temperature. The activation energy (E_a), was calculated from the Arrhenius plot of ln R *vs* 1000/T. Arrhenius plot shows that the activation energies of the removal are

positive and equal to 4.79 and 4.32 kJ/mole for $Sr_3NbO_{5.5}$ and $BaSr_2NbO_{5.5}$ respectively. The activation energy of the removal was –0.018 kJ/mole for $Ba_2SrNbO_{5.5}$. This reflects the differences in the strength of the interaction forces between the dye and the oxides.

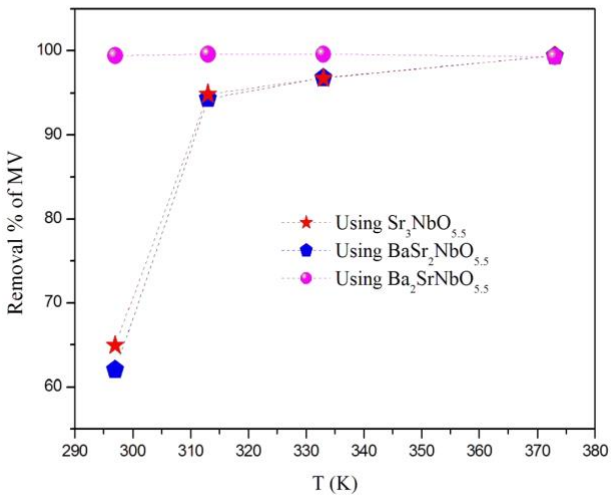

Fig. 5. the effect of temperature on the MV removal. The time, volume, pH and concentration of dyes solutions are 150 min, 50 mL, 5.1 and 10 ppm, respectively.

Effect of pH

The pH of solutions is a key parameter in dye adsorption. The magnitude of electrostatic charges which are impacted by the ionized dye molecules is controlled by the solution pH. As a result, the rate of adsorption will vary with the pH of the medium used. In general, at low solution pH, the percentage of dye removal will decrease for cationic dye adsorption, while for anionic dyes the percentage of removal will increase. This is due to the increase in the positive charge on the solution interface and the adsorbent surface. In contrast, high solution pH is preferable for cationic dye adsorption but shows a lower efficiency for anionic dye adsorption. The positive charge at the solution interface will decrease while the adsorbent surface appears negatively charged.

To study the effect of pH, experiments were carried out at various pH values, ranging from 1 to 10 for constant dye concentration (10 ppm) and adsorbent mass (0.1 g). Figure 6 presents the removal of dyes as a function of pH. It was observed that the removal of MV using the doped oxides increases as pH increased. The highest removal of MV was recorded at pH = 10 around 98.8 % using $Ba_2SrNbO_{5.5}$ where the lowest removal of MV was recorded at pH = 4 around 22 % using the same oxide. The removal of MV using $Sr_3NbO_{5.5}$ has gradually increased from ~50 % to ~75 % as pH increased from 1 to 10. The removal of MV reached

maximum (~91 %) using $BaSr_2NbO_{5.5}$ at pH 1 and 10. The removal efficiency of the adsorbents is clearly increased as the acidity decreased.

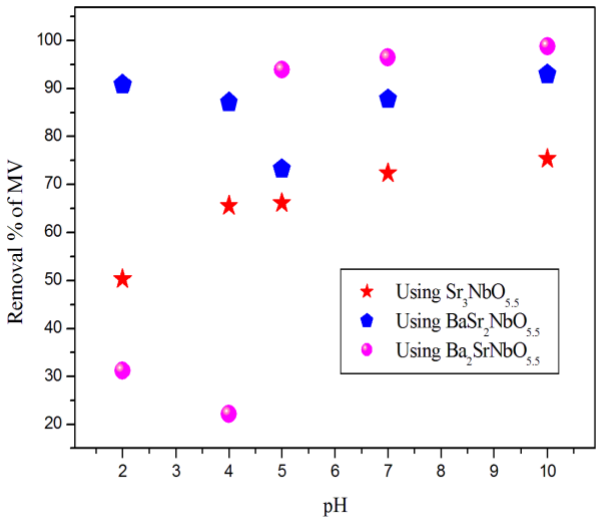

Fig. 6. The effect of pH on the removal of MV. The time, volume and concentration of dyes solution are 150 min, 50 mL, and 10 ppm, respectively.

CONCLUSION

The removal of methyl violet from aqueous solution using the A-site doped perovskites $Ba_xSr_{3-x}NbO_{5.5}$ has been reported. The nano particle oxides were synthesized by solid state reaction and characterized by XRD. The results showed that the substitution of Ba^{2+} has influenced both the texture and adsorption properties of the oxides. It was found that the adsorbent amounts of organic dye increase as the Ba^{2+} content increased. The removal of MV increases as the physical parameters: time, temperature, pH, adsorbent mass increased. The maximum capacities of adsorbent are 46.47, 13.09 and 8.03 mg/g for $Ba_2SrNbO_{5.5}$, $BaSr_2NbO_{5.5}$ and $Sr_3NbO_{5.5}$, respectively. The highest removal efficiency was recorded for MV dye using $Ba_2SrNbO_{5.5}$ at pH = 10, where the lowest removal was observed for the same oxide at pH = 2.

REFRENCES

1. ANIMITSA, I., A. NEIMAN, N. KOCHETOVA, D. KORONA, A. SHARAFUTDINOV, Chemical diffusion of water in the double perovskites $Ba_4Ca_2Nb_2O_{11}$ and $Sr_6Ta_2O_{11}$, *Solid State Ionics*, 2006, **177**, 2363–2368.

2. ANIMITSA, I., A. NEIMAN, A. SHARAFUTDINOV, S. NOCHRIN, Strontium tantalates with perovskite-related structure, *Solid State Ionics*, 2001, **136–137,** 265–271.
3. BONETTO, L.R., F. FERRARINI, C. DE MARCO, J.S. CRESPO, R. GUÉGAN, M. GIOVANELA, Removal of methyl violet 2B dye from aqueous solution using a magnetic composite as an adsorbent, *Journal of Water Process Engineering*, Elsevier, 2015, **6**, 11–20.
4. EMAN, A., Perovskite synthesis, properties and their related biochemical and industrial application, *Saudi Pharmaceutical Journal*, 2019**, 27**, 817–829
5. FERGUS, J.W., Perovskite oxides for semiconductor-based gas sensors, *Sensors and Actuators B: Chemical*, 2007, **2**, 1169–1179.
6. HENG, G., C. HAIYUAN, Z. HAIYAN, H. XU, Y. JIAN, Low-temperature processed yttrium-doped $SrSnO_3$ perovskite electron transport layer for planar heterojunction perovskite solar cells with high efficiency, *Nano Energy* 2019**, 59**, 1–9.
7. ISHIHARA, T., Structure and properties of perovskite oxides, in: *Perovskite Oxide for Solid Oxide Fuel Cells*, T. Ishihara ed., Springer, US, 2009, pp. 1–16.
8. KING, G., P.M. WOODWARD, Cation ordering in perovskites, *Journal of Materials Chemistry*, 2010, **28,** 5785–5796.
9. LANGFORD, J.I., A.J.C. WILSON, Scherrer after sixty years: A survey and some new results in the determination of crystallite size, *Journal of Applied Crystallography*, 1978, **2,** 102–113.
10. LECOMTE, J., J.P. LOUP, M. HERVIEU, B. RAVEAU, Non-stoichiometry and electrical conductivity of strontium niobates with perovskite structure, *Physica Status Solidi*, 1981, **2**, 743–752.
11. NOGI, K., M. HOSOKAWA, M. NAITO, T. YOKOYAMA (eds), *Nanoparticle Technology Handbook*, Elsevier, 2012.
12. SHANNON, R.D., Revised effective ionic-radii and systematic studies of interatomic distances in halides and chalcogenides, *Acta Crystallographica Section A*, 1976, **32**, 751–767.
13. SMYTH, D.M., Defects and order in perovskite-related oxides, *Annual Review of Materials Science*, 1985, **1**, 329–357.
14. SOMESHWAR, P., G. RAMESH, Significant role of perovskite materials for degradation of organic pollutants, https://www.intechopen.com/online-first/significant-role-of-perovskite-materials-for-degradation-of-organic-pollutants, April 3rd, 2020, DOI: 10.5772/intechopen. 91680
15. TEJUCA, L.G., J.L.G. FIERRO (eds.), *Properties and Applications of Perovskite-Type Oxides (Chemical Industries)*, Taylor & Francis, 1992.
16. WANG, S., Y. BOYJOO, A. CHOUEIB, Z.H. ZHU, Removal of dyes from aqueous solution using fly ash and red mud, *Water Research*, 2005**, 39**, 129–138.
17. WILES, D.B., R.A. YOUNG, A new computer program for Rietveld analysis of X-ray diffraction patterns, *Journal of Applied Crystallograph*y, 1981, **14,** 149–151.
18. *********Articles on Triarylmethane Dyes, Including: Phenolphthalein, Methyl Violet, Bromothymol Blue, Coomassie Brilliant Blue, Bromophenol Blue, Malachite Green, Thymolphthalein, Triphenylmethane, Fuchsine, New Fuchsine, Fuchsine Acid, Phenol Red*, Hephaestus Books, 2011.